NASA/TM—20220001877

Displacement Damage Test Report for the OMT1090 Optical Switch

Thomas A. Carstens

Anthony M. Phan

Michael J. Campola

Landen D. Ryder

Jean-Marie Lauenstein

Alexandre LeRoch

February 2022

NASA STI Program Report Series

The NASA STI Program collects, organizes, provides for archiving, and disseminates NASA's STI. The NASA STI program provides access to the NTRS Registered and its public interface, the NASA Technical Reports Server, thus providing one of the largest collections of aeronautical and space science STI in the world. Results are published in both non-NASA channels and by NASA in the NASA STI Report Series, which includes the following report types:

- TECHNICAL PUBLICATION. Reports of completed research or a major significant phase of research that present the results of NASA Programs and include extensive data or theoretical analysis. Includes compilations of significant scientific and technical data and information deemed to be of continuing reference value. NASA counterpart of peer-reviewed formal professional papers but has less stringent limitations on manuscript length and extent of graphic presentations.

- TECHNICAL MEMORANDUM. Scientific and technical findings that are preliminary or of specialized interest, e.g., quick release reports, working papers, and bibliographies that contain minimal annotation. Does not contain extensive analysis.

- CONTRACTOR REPORT. Scientific and technical findings by NASA-sponsored contractors and grantees.

- CONFERENCE PUBLICATION. Collected papers from scientific and technical conferences, symposia, seminars, or other meetings sponsored or co-sponsored by NASA.

- SPECIAL PUBLICATION. Scientific, technical, or historical information from NASA programs, projects, and missions, often concerned with subjects having substantial public interest.

- TECHNICAL TRANSLATION. English-language translations of foreign scientific and technical material pertinent to NASA's mission.

Specialized services also include organizing and publishing research results, distributing specialized research announcements and feeds, providing information desk and personal search support, and enabling data exchange services.

For more information about the NASA STI program, see the following:

- Access the NASA STI program home page at http://www.sti.nasa.gov

- Help desk contact information:

https://www.sti.nasa.gov/sti-contact-form/
and select the "General" help request type.

NASA/TM—20220001877

Displacement Damage Test Report for the OMT1090 Optical Switch

Thomas A. Carstens
Goddard Space Flight Center, Greenbelt, MD

Anthony M. Phan
Science Systems and Applications (SSAI), Inc., Lanham MD

Michael J. Campola
Goddard Space Flight Center, Greenbelt, MD

Landen D. Ryder
Goddard Space Flight Center, Greenbelt, MD

Jean-Marie Lauenstein
Goddard Space Flight Center, Greenbelt, MD

Alexandre LeRoch
Universities Space Research Association, Columbia, MD

Test Date: 10/1/2021
Report Date: 1/12/2022

National Aeronautics and
Space Administration

Goddard Space Flight Center
Greenbelt, MD 20771

February 2022

Acknowledgments (optional)

This work was sponsored by the NASA GSFC Radiation Effects and Analysis Group and supported by the On-Orbit Servicing, Assembly and Manufacturing (OSAM-1) mission.

Level of Review: This material has been technically reviewed by technical management.

Available from

NASA STI Program
Mail Stop 148
NASA's Langley Research Center
Hampton, VA 23681-2199

National Technical Information Service
5285 Port Royal Road
Springfield, VA 22161
703-605-6000

This report is available in electronic form at

https://radhome.gsfc.nasa.gov/

I. Introduction

The purpose of this study was to examine the displacement damage susceptibility of the OMT1090 optical switch manufactured by TT Electronics / OPTEK Technology Inc. and compare it to the results of the OPB847TXV.

II. Device Description

The OMT1090 is a 50V slotted optical switch with a gallium aluminum arsenide LED and a silicon phototransistor. Phototransistor switching takes place when an opaque object passes through the slot. Table I shows the test and part details. Figure 1 shows the pin configuration of the PCB mounted package. The device performance specifications can be found in the manufacturer's datasheet [1].

Table I
Test and part information.

Generic Part Number	OMT1090
REAG ID	21-012
Manufacturer	TT Electronics / OPTEK Technology Inc.
Lot/Date Code	M2047
Quantity tested	10
Part Function	Optical switch
Package Style	PCB mount
Test Engineer	Anthony Phan
Test Equipment	Keithley SMU

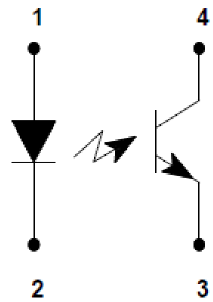

Pin #	Description
1	Anode
2	Cathode
3	Emitter
4	Collector

Fig. 1. Pin configuration and description.

III. Test Method

A. Irradiation Procedure

The irradiation was performed at Crocker Nuclear Laboratory on the campus of The University of California at Davis with a proton energy of 64 MeV. Figure 2 and Figure 3 shows the bias circuit during radiation. Table II shows the fluence and total dose steps for each exposure. Five devices were irradiated under bias and five were unbiased. There were two control devices. DUTs 2, 3, 4, 10, and 5 were biased. DUTs 1, 6, 7 ,8, and 9 were unbiased. Finally, DUTs 11 and 12 were used as controls.

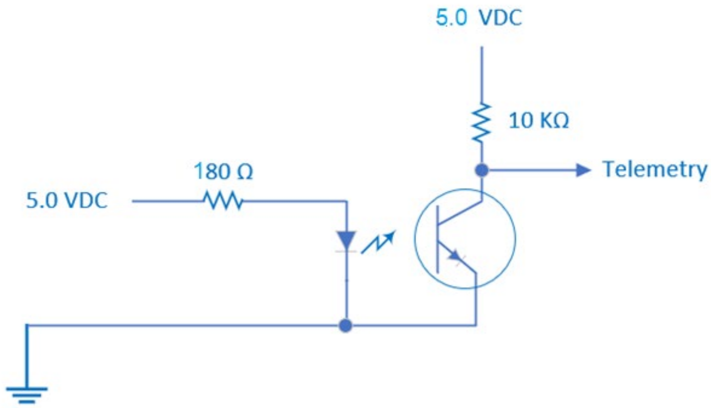

Fig. 2. Schematic diagram of the irradiation bias configuration.

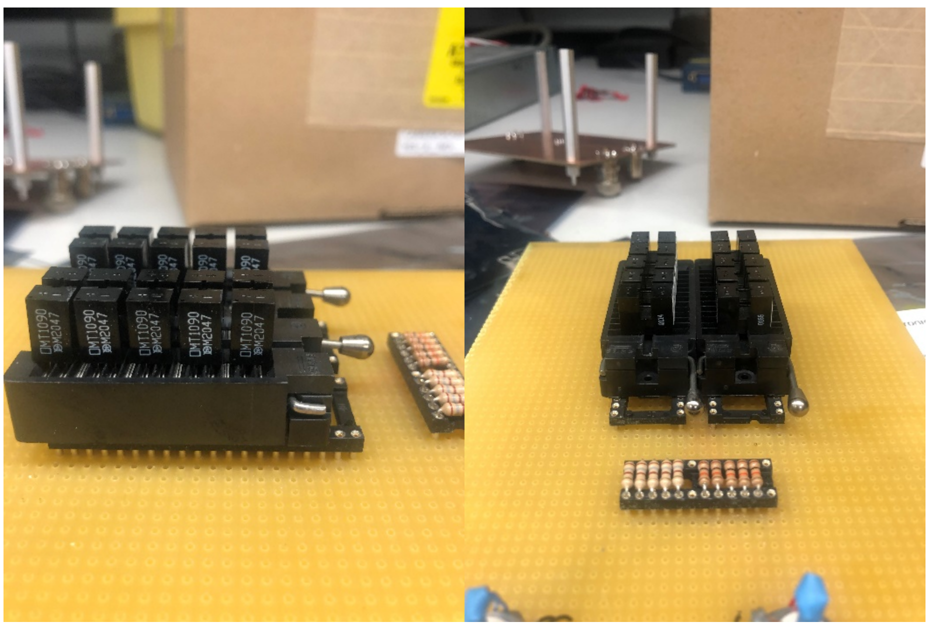

Fig. 3. Bias board and optical switches.

Table II
Fluence and total dose for each exposure.

Run Number	Total Dose (krad(Si))	Per Run Fluence (#/cm^2)	Total Fluence (#/cm^2)
1	4	3.01E+10	3.01E+10
2	6	1.51E+10	4.52E+10
3	7	3.77E+10	5.27E+10
4	8	2.26E+10	6.02E+10
5	10	5.27E+10	7.53E+10
6	12	3.77E+10	9.04E+10

B. Test Conditions

Test temperature: Room temperature

Test Parameters: 10V was applied at V_{CE} while the current was swept through the LED and forward voltage measured. The remaining parameters were measured using the datasheet's test conditions, see Table III.

Measurements: Forward voltage, Emitter-Collector Breakdown Voltage, Collector-Emitter Breakdown Voltage, On-state Collector Current, Collector-Emitter Saturation Voltage

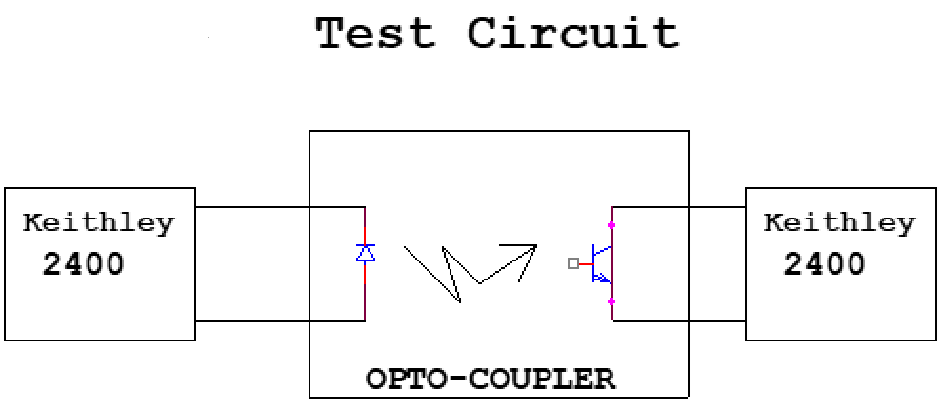

Fig. 4. Schematic diagram of the test circuit.

Table III
List of parameters measured.

Symbol	Parameter	MIN	TYP	MAX	Units	Test Conditions
V_F	Forward Voltage	1	1.35	1.7	V	$I_F = 20$ mA
$V_{(BR)CEO}$	Collector-Emitter Breakdown Voltage	50	110		V	$I_C = 1$ mA, $I_F = 0$
$V_{(BR)ECO}$	Emitter-Collector Breakdown Voltage	7	10		V	$I_E = 100$ uA, $I_F = 0$
I_{CEO}	Collector-Emitter Dark Current			200	nA	$V_{CE} = 20$ V, $I_F = 0$
$I_{C(ON)}$	On-state Collector Current	4			mA	$V_{CE} = 10$ V, $I_F = 20$ mA
$V_{CE(SAT)}$	Collector-Emitter Saturation Voltage			0.4	V	$I_C = 2$ mA, $I_F = 20$ mA

IV. Results

It should be noted that these optical switches contain large part-to-part variability. DUT 11 and DUT 12 had their collector-emitter voltage swept over a range of voltages. In addition, two different forward LED currents were used. The collector currents for the control DUTs were divergent after one volt for both the 20mA and 30mA LED forward current cases. Ideally the collector current for each LED forward current case should overlap for each DUT. The curves should be independent of the DUT. This is demonstrated in Figure 5 below.

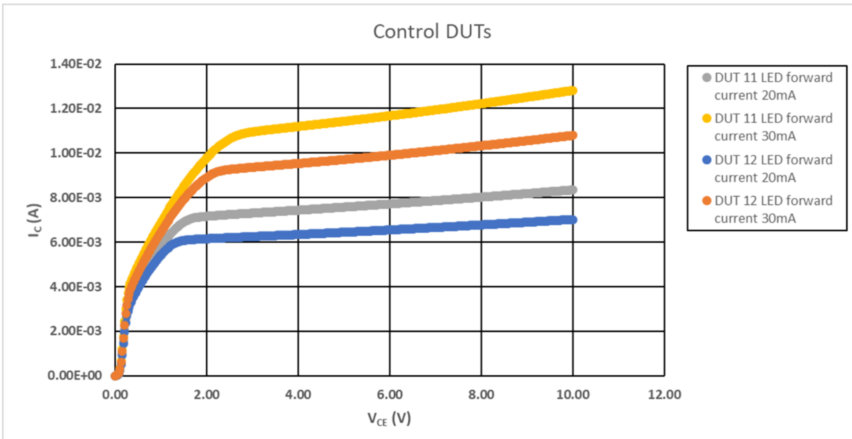

Fig. 5. Collector-Emitter Voltage (V) vs. Collector Current (A)

The forward voltage was un-affected by the dose for the biased and unbiased cases. This is shown in Figure 6. Figure 7 and Figure 8 show the Collector-Emitter Breakdown Voltage ($V_{(BR)CEO}$) and the Emitter-Collector Breakdown Voltage ($V_{(BR)ECO}$). The $V_{(BR)CEO}$ remained constant for the unbiased case. However, the $V_{(BR)CEO}$ of the biased case went out of specification after a dose of 6 krad(Si) (64 MeV equivalent fluence of 4.52×10^{10} protons/cm^2). In particular, DUT (2) failed after 6 krad(Si). The $V_{(BR)ECO}$ increased slightly with dose for unbiased case but stayed above the specification minimum. On the other hand for the biased case the $V_{(BR)ECO}$ failed after a dose of 6 krad(Si) (64 MeV equivalent fluence of 4.52×10^{10} protons/cm^2). This was caused by DUT 2 failing.

After the first irradiation step, the on-state collector current ($I_{C(ON)}$) saw a significant decrease. At a dose of 6 krad(Si) (64 MeV equivalent fluence of about 4.52×10^{10} protons/cm^2), $I_{C(ON)}$ was below specification according the design application of 1mA. This is shown in Figures 9 and 10. Once again the first DUT 2 was the first to fail. This can be seen again in Figures 11 and 12. Figure 11 shows that all DUTs' collector currents were above the application minimum of 1mA after 6 krad(Si). However, according to Figure 12 after 7 krad(Si) it can be seen that DUT 2 has a significant drop in the collector current. In addition, DUT 6 is slightly below the application minimum for the collector current after 7 krad(Si).

In summary the optical switches showed variability before irradiation. This variability was only exacerbated by dose effects. The optical switches are composed of both a photodiode and phototransistor. Based on the test results radiation negatively impacts the phototransistor more than the photodiode. The first device to fail was DUT 2, which was biased. It was able to function until a dose of 6 krad(Si) or 64 MeV equivalent fluence of 4.52×10^{10} protons/cm^2.

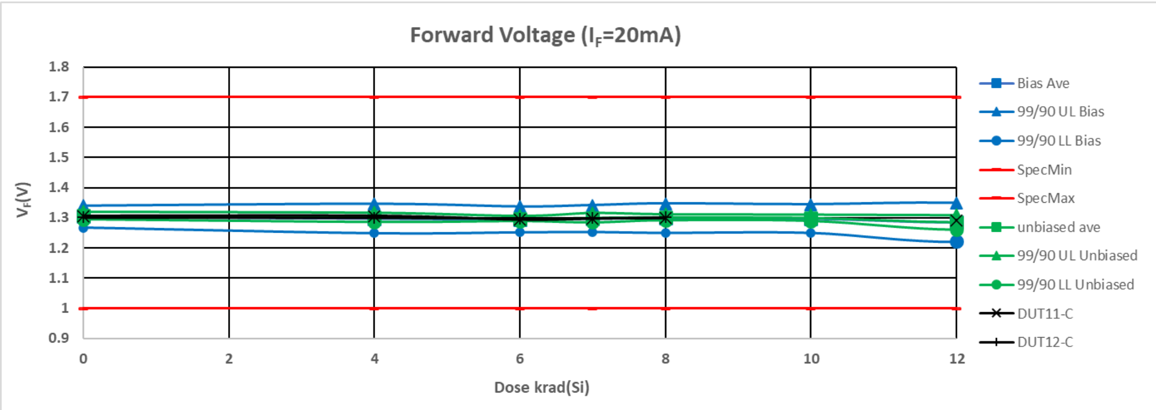

Fig. 6. Forward Voltage (V) vs. Dose (krad(Si))

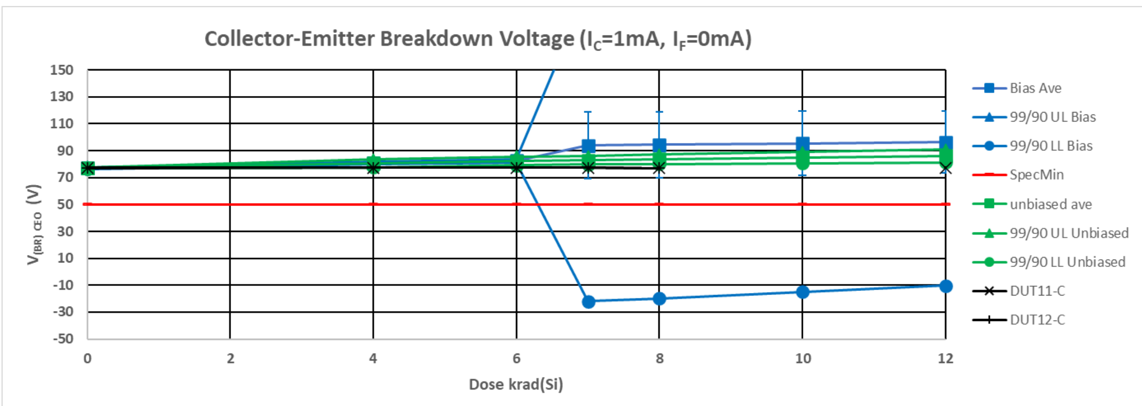

Fig. 7. Collector-Emitter Breakdown Voltage (V) vs. Dose (krad(Si))

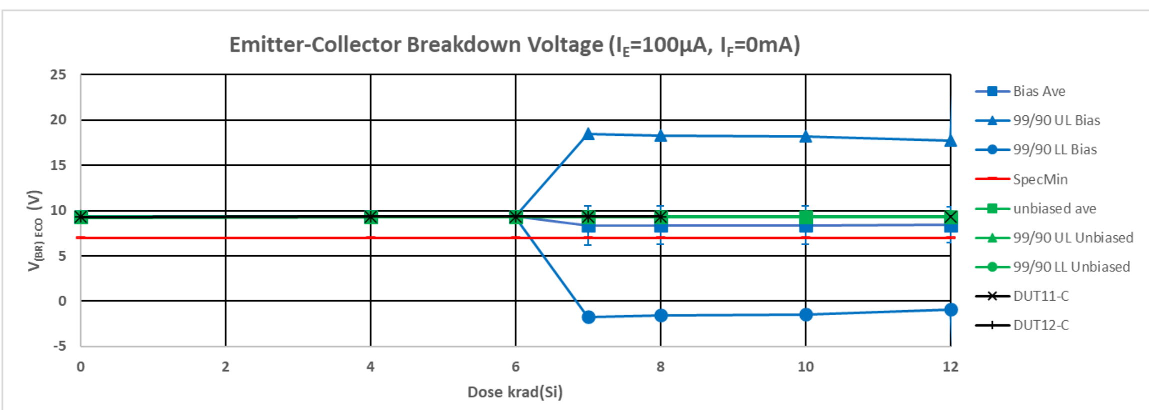

Fig. 8. Emitter-Collector Breakdown Voltage (V) vs. Dose (krad(Si))

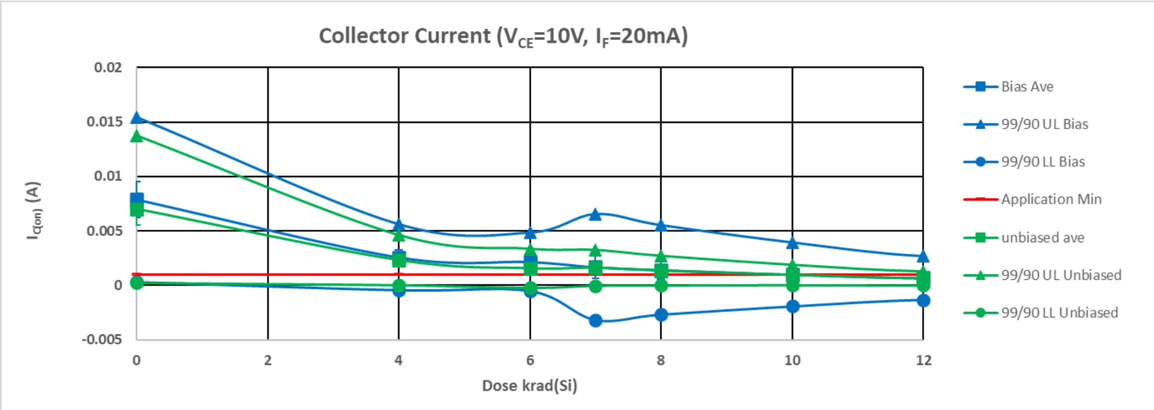

Fig. 9. Average On-state Collector Current (A) vs. Dose (krad(Si))

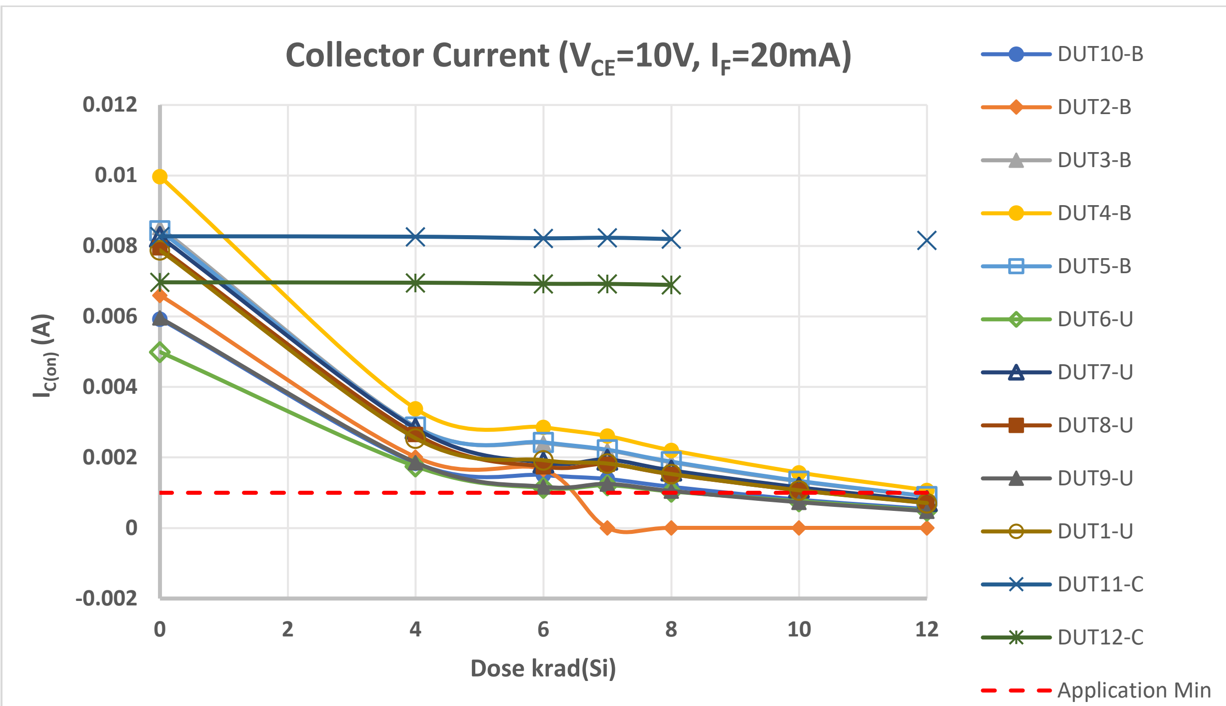

Fig. 10. On-state Collector Current (A) vs. Dose (krad(Si)) for each DUT

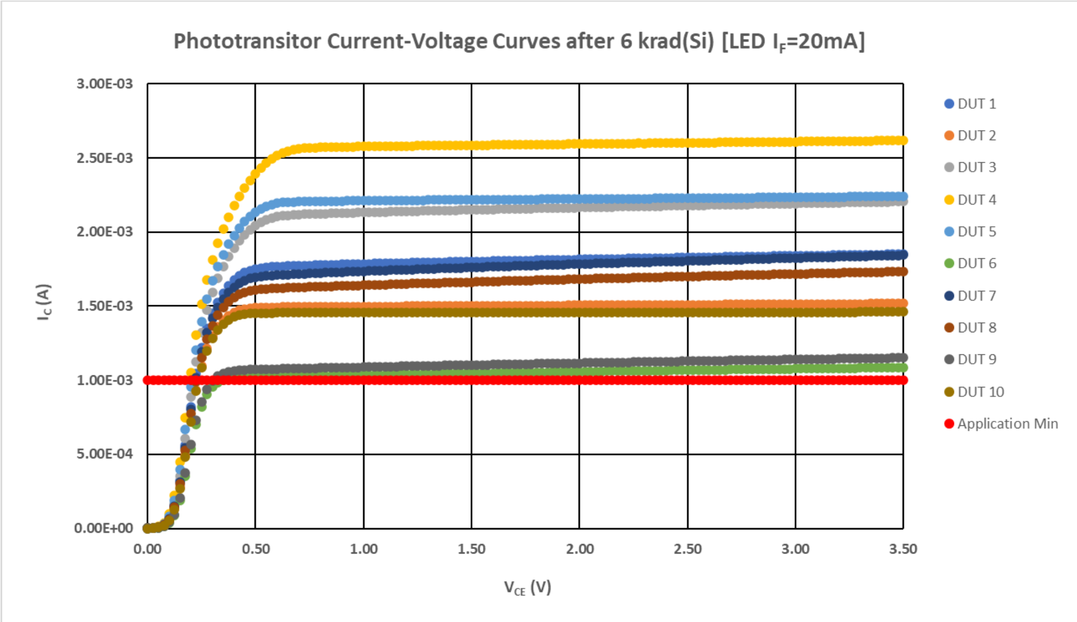

Fig. 11. Collector Current (A) vs. Collector-Emitter Voltage (V) after 6 krad(Si)

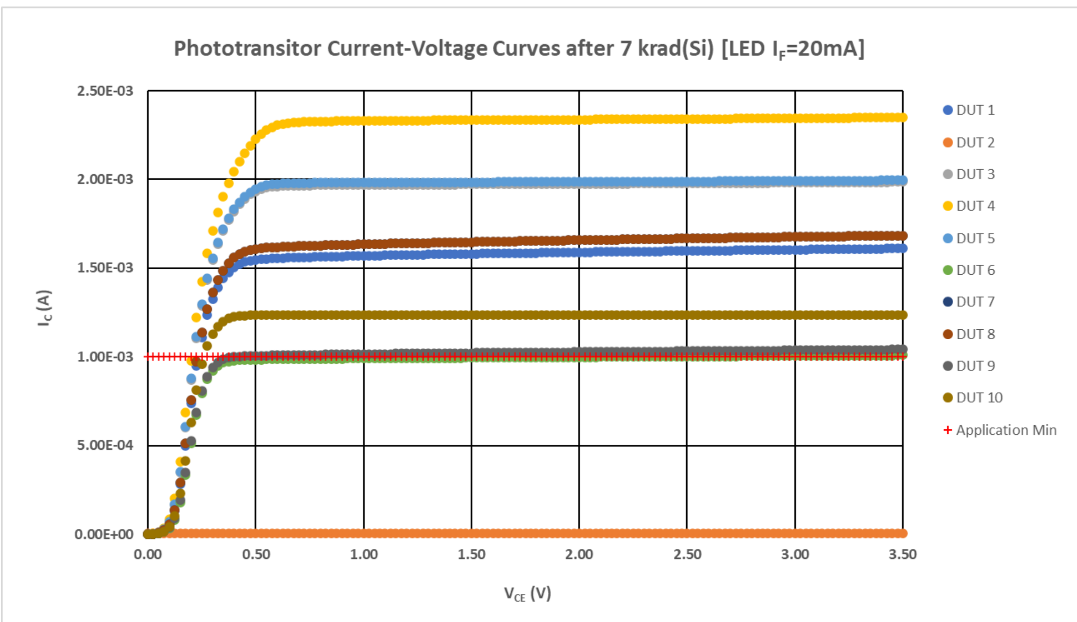

Fig. 12. Collector Current (A) vs. Collector-Emitter Voltage (V) after 7 krad(Si)

In addition, the data from the OMT1090 optical switch was combined with the data from the OPB847 optical switch. The data was combined because OMT1090 is serving as a replacement part for the OPB847. The combined data analysis can be seen below in Figures 13-16. Many of the same conclusions from OMT1090 can be reached with the combined analysis. The main benefit of combining the data sets was to increase the sample size which helps improve the 99/90 statistics. This can be seen when comparing the unbiased collector current in Fig 9 and Fig 16. In Fig. 9 the lower limit of the 99/90 unbiased average is below the application minimum for all doses. However, in Fig.16 the lower limit of 99/90 unbiased average is above the application minimum until 4 krad(Si).

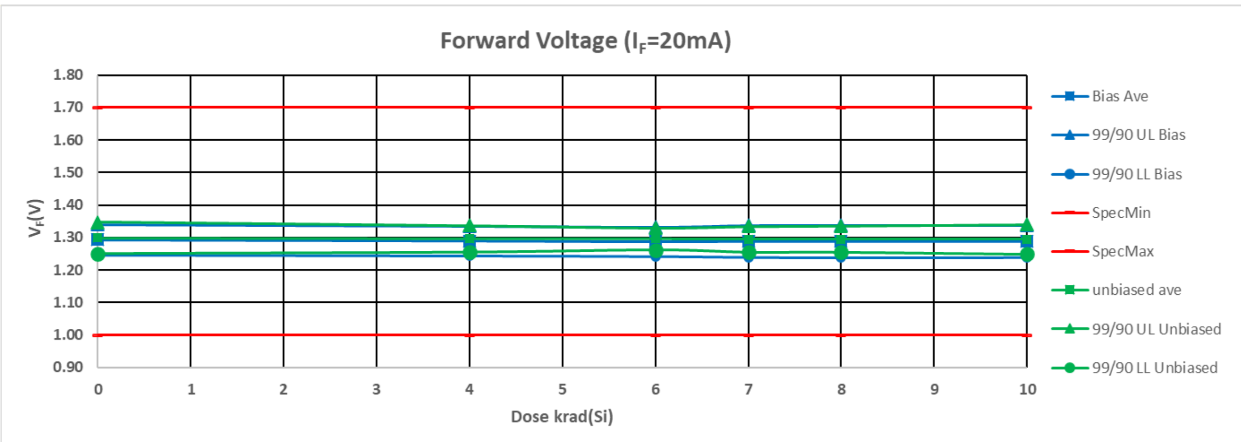

Fig. 13. Combined OPB847 and OMT1090, Forward Voltage (V) vs. Dose (krad(Si))

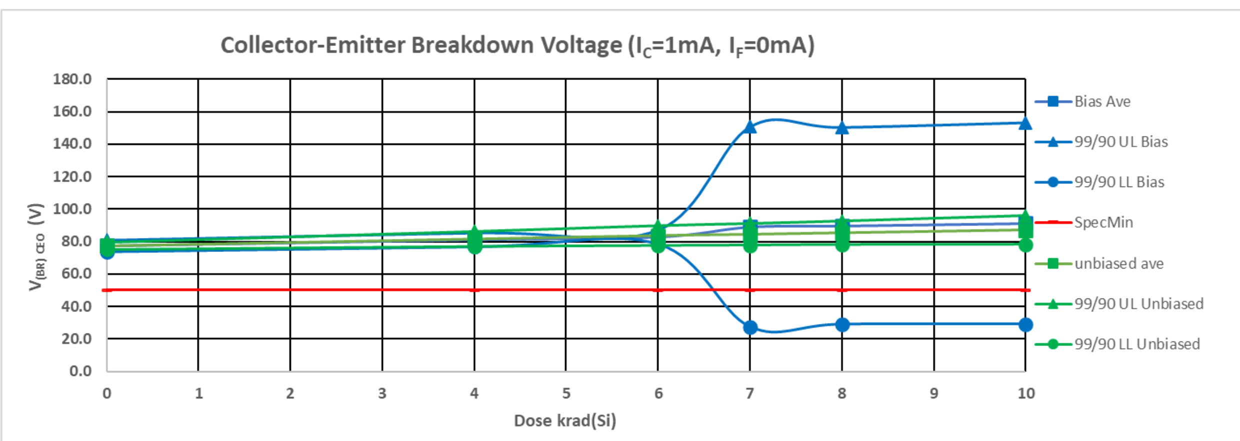

Fig. 14. Combined OPB847 and OMT1090, Collector-Emitter Breakdown Voltage (V) vs. Dose (krad(Si))

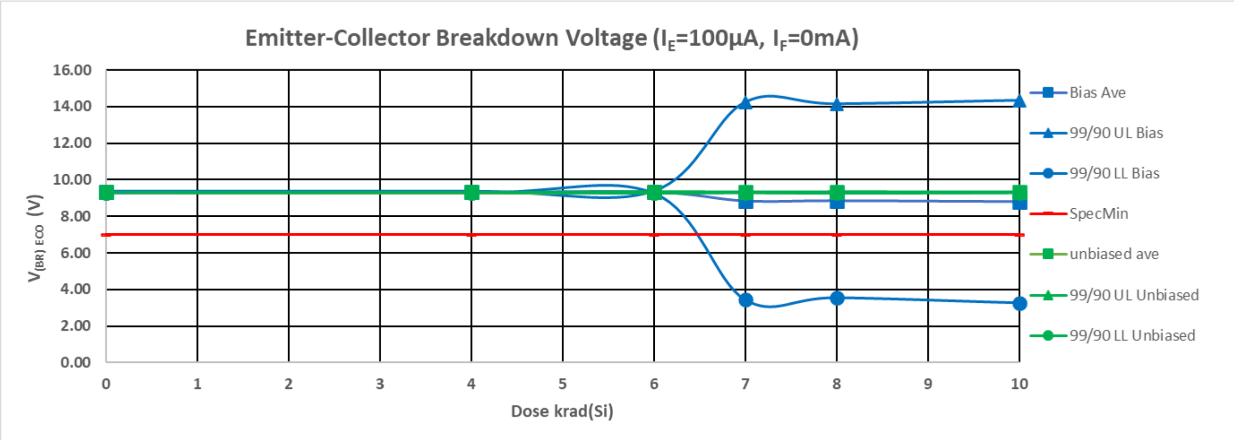

Fig. 15. Combined OPB847 and OMT1090, Emitter-Collector Breakdown Voltage (V) vs. Dose (krad(Si))

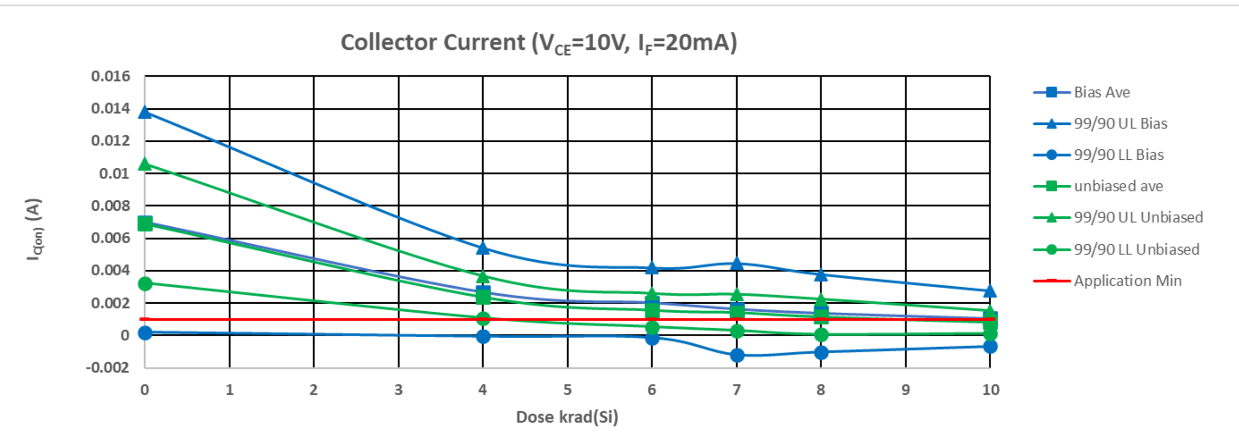

Fig. 16. Combined OPB847 and OMT1090, Average On-state Collector Current (A) vs. Dose (krad(Si))

V. Summary

The OMT1090 showed large part to part variability before dose. Radiation exacerbated this part to part variability. Radiation negatively impacts the phototransistor more than the photodiode.

VI. Reference

[1] TT Electronics / OPTEK Technology, Inc., “Slotted Optical Switch” OMT1090, OMT1090 datasheet, 3/20

[2] OPTEK Technology, Inc., “Slotted Optical Switch” OPB847, OPB848 datasheet, 7/09 [Rev. A.1]